ORIGINAL RESEARCH PAPER



A non-contact gap measurement method for narrow and irregular targets using inductive planar sensors with simple calibration

Dian Jiao | Liwei Ni | Xueyang Yu | Jiang Zhe

Department of Mechanical Engineering, University of Akron, Akron, Ohio, USA

Correspondence

Dr. Jiang Zhe, Department of Mechanical Engineering, The University of Akron, 302 Buchtel Commons, Akron, OH 44325-3903, USA.

Email: jzhe@uakron.edu

Funding information

This work was partially supported by NSF Awards #1940879 of USA.

Abstract

Planar inductive sensors are widely used for non-contact gap measurement. Usually, a change in size, shape, or material of the target requires a tedious recalibration of the measurement setup. This paper aims to present a new method to measure the gap from irregular and narrow targets using a planar inductive sensor without this tedious calibration process. The magnetic field distribution on this target was numerically studied, and the findings suggested that a simpler calibration would work by modeling the induced current in the target as a virtual planar coil. For this target, we found that the calibration curves corresponding to different materials can be obtained by adding a constant C to the base curve. To validate this approach, three planar coils of different sizes were tested with four metallic turbine blade-shaped targets. Results showed that the measured gaps matched well with the real gaps, with a maximum error of about 3.703%. The new approach can be applied to various applications including 3D printer build platform calibration, bandsaw blade deviation detection, and blade tip clearance monitoring.

1 | INTRODUCTION

Planar inductive sensors have been utilized in a variety of applications such as the measurements of gaps, thicknesses, and surface treatments [1, 2]. Benefitting from their working principle, inductive sensors exhibit excellent performance in wet, dirty, and high-temperature environments [3], and they provide reliable, non-contact gap measurements with micro and nano metre resolutions [4].

Traditionally, gap measurement depends on the establishment of a calibration curve between the inductance variation of the planar coil and the gap. This curve is usually established by using a target whose surface is at least twice as large as the outer diameter of the sensing coil [5-7]. When the target is narrower than the sensing coil, one has to either use a smaller sensor, or recalibrate the sensor with the new object since the eddy current will be different. Furthermore, if the target material is changed, the calibration curve will also need to be rebuilt in order to reflect the conductivity change. Therefore, a set of calibration curves corresponding to various materials needs to be established for an inductive sensor, which is undoubtedly a tedious and complex process. To address

this problem, Tian et al. proposed that the effect of different target materials on the calibration curve can be reduced by increasing the excitation frequency of the inductive sensor [8]. However, using a high excitation frequency (e.g. 5 MHz or higher) significantly increases the amount of data, and therefore processing time, while the material's effect still cannot be completely eliminated. Yating et al. developed a new eddy current gap measuring instrument, which is independent of sample electromagnetic properties [9]. Although the influence of changes in a target material can be somewhat eliminated using a coil impedance vector projection approach, a roughly 13% error in the 0.1-0.2 mm gap measurement range was found when using aluminum and a copper plate targets. Recently Wang et al. developed a method where the gap measurement is made independent of the target's conductivity by shifting the calibration curve for a different material with an offset value [10]. While this method is based on calculating the geometry of the superconductor image plane, the conductivity of each material needs to be measured precisely. Recently Jiao et al. proposed a method using mutual inductance calculations to simplify the calibration when measuring gaps from infinite plate targets [11]. However, all of the previously mentioned methods

This is an open access article under the terms of the Creative Commons Attribution License, which permits use, distribution and reproduction in any medium, provided the original work is properly cited.

© 2021 The Authors. IET Science, Measurement & Technology published by John Wiley & Sons Ltd on behalf of The Institution of Engineering and Technology

wileyonlinelibrary.com/iet-smt IET Sci. Meas. Technol. 2021;15:710–718.

[8-11] are only valid for gap measurements from infinite plate targets.

Nevertheless, many industrial applications require precision when measuring gaps from narrow and irregular objects. In 3D printing, when a task requires the changing of printing material, the build platform (i.e. thin metallic plates where the material is printed) needs to be replaced since the process of printing various materials requires different adherences and thermal conductivities [12]. For instance, a titanium platform is used for high-temperature printing, while a copper platform is used for uniform heat dissipation when a large object is printed [13]. To guarantee the printing process starts and ends at the designed locations, there is a critical need to monitor X, Y, and Z positions with high accuracy before and after the replacement of the build platforms [14]. Currently, there is no low-cost sensor that can detect the accurate position of a thin build platform made of different materials [15]. Similarly, precise position monitoring is necessary for bandsaw blade deviation when a replacement bandsaw blade made of different materials is required for the cutting of various materials [16, 17]. In fan blade tip clearance monitoring, dynamic tip clearance needs to be measured in real time with a resolution of $\approx 10 \,\mu\text{m}$ to ensure safe operation [18]. Fan blade width could be smaller than the sensing coil and usually cannot be considered as an infinite plate target. When there is a need to increase the thrust or power in a harsh environment, the most common way is to change the blade material from aluminum alloy to titanium alloy, which has higher strength and corrosion/creep resistance [19, 20]. The above applications all need a high resolution (e.g. 10-20 μ m) monitoring of gaps or locations of targets with abnormal geometries. Planar inductive sensors could play an indispensable role in these applications because of their simplicity, low cost, and robustness. Thus, it is necessary to develop a gap measurement method used for targets with a typical geometry using planar inductive sensors of any size that only requires simple calibration and gives sufficient measurement accuracy.

In this paper, a new approach to measure the gap from irregular and narrow targets is developed using a planar inductive sensor of any size, with the aim of simplifying the calibration process. The finite element method (FEM) simulation was conducted to prove a new assumption used in the model. Test results have validated the new approach to measuring the gap from various targets with concise calibration and high accuracy.

2 | WORKING PRINCIPLE

The working principle of the gap measurement from a narrow target using a planar sensing coil is shown in Figure 1. A magnetic field is induced by an AC excitation applied to the sensing coil, causing an eddy current to appear on the target surface. To analyse the distribution of eddy current on the target, the finite element analysis (FEA) was first conducted on a narrow, rectangular target shown in Figure 1(a). The magnetic flux density mapped onto the target shows that the eddy current is distributed on the top surface and extends down the side surfaces, such that if they were folded up to the same plane it

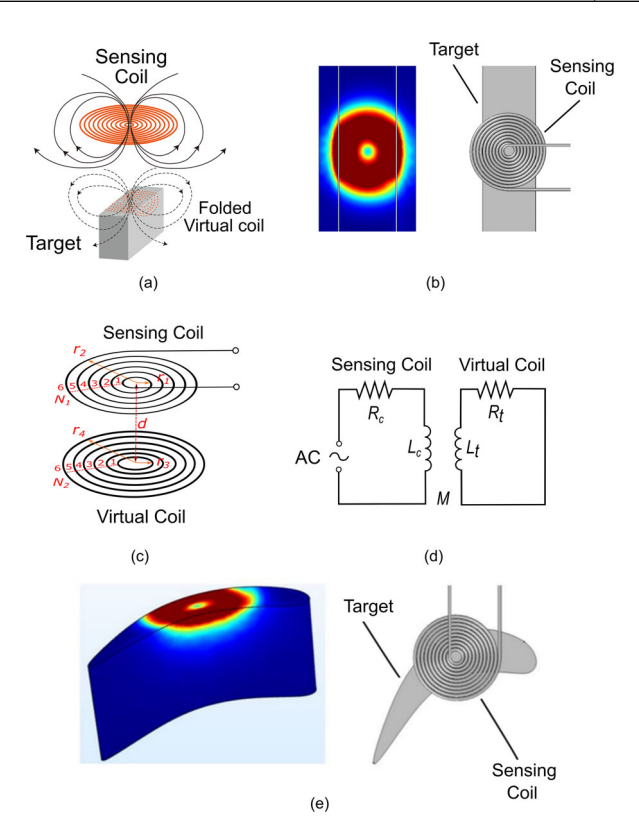


FIGURE 1 Working principle and simulations of the gap measurement for a narrow target (a) Schematic sketch of the working principle of the gap measurement for a narrow target. (b) Simulated magnetic flux density distribution when flipping the side surface to the top surface by finite element analysis. (c) Gap measurement can be modeled as the configuration of two coaxial planar coils, namely, a sensing coil (top) and a virtual coil (bottom). (d) Equivalent circuit of a coil-to-coil system. (e) Magnetic flux density distribution on the blade target

would create a circle (see details of the FEM simulation in the Supporting Information). Figure 1(b) shows the top view of a typical magnetic flux density distribution on the side surface is flipped to the top surface. The magnetic flux density mapping on a more complex target, a turbine blade-shaped object, was also simulated. Figure 1(e) shows the magnetic flux distribution in the blade-shaped target. The magnetic flux details are shown in the Supporting Information. These simulations suggest that the eddy current in an irregular and narrow target can be approximately modeled as a virtual planar circular coil. It is worth noting that the previous studies indicate that the eddy current distribution in an infinite plate target can be regarded as an array of ring loops [21, 22]. Furthermore, Paese et al. proved that a set of ring loops can be used to mathematically model a planar circular coil [23]. Details of the FEM simulations are provided in the Supporting Information. Thus, the coil-to-coil model can be established to analyse the mutual inductance between the sensing and virtual coils, as shown in Figure 1(c), where r_1 , r_2 , r_3 , and r_4 are the inner and outer radii, d is the gap between the sensing and virtual coils, and N_1 and N_2 are the turn numbers of the two planar coils [22]. The sensing coil has the resistance R_C and the inductance L_C . Similarly, the virtual coil is modeled as a self-relative inductance L_t in series with a

resistance R_t (as shown in Figure 1(d)). The equivalent circuit of the coil-to-coil system is shown in Figure 1(d) [21].

The equivalent inductance (L) of the sensing coil can be expressed as the equation [24]:

$$L = L_C - \frac{\omega^2 M^2 L_t}{R_t^2 + \omega^2 L_t^2}$$
 (1)

where M represents the mutual inductance between the two coils, and ω refers to the angular frequency of the excitation signal. M, L_t , and R_t in Equation (1) can be expressed as the functions of the gap d, inner and outer radii, and turn numbers of the two coils [25–27]:

$$M = g(r_1, r_2, r_3, r_4, d, N_1, N_2)$$
 (2)

$$L_t = h(r_3, r_4, N_2)$$
 (3)

$$R_t = y(r_3, r_4, N_2)$$
 (4)

The details of Equations (2), (3), and (4) are described in [11, 25, 28]. L_t refers to the function of N_2 (virtual planar coil turn numbers), r_3 and r_4 , and d (gap distance), and changing N_2 can generate the same variations of L_t as changing r_3 and r_4 . Hence, we assume r_3 equals r_1 , and r_4 equals r_2 . Note that the FEA simulation of the narrow rectangular object and the turbine blade confirmed the reasonability of this assumption (see Supporting Information). Further FEA simulation showed that the eddy current distribution remains nearly unchanged when the gap "d'' varies within a small range (d from 0.05 to 0.5 times of the sensing coil size r_2), indicating that the geometry of the virtual coil (r_3 , r_4) can be treated as a constant in calculations [21]. Thus, Equation (1) can be simplified as [28, 29]:

$$L = L_C - f(r_1, r_2, d, N_1, N_2)$$
 (5)

In Equation (5), r_1 , r_2 and N_1 (the geometry of the sensing coil) are known, while the gap d and N_2 are unknown d and N_1/N_2 relations can be established by measuring the sensing coil inductance (L) at 5–6 different gaps [11]. Once the relation between the two coils turn ratio and the gap is established, gap d can be calculated based on Equation (5) with the measured sensing coil inductance L.

3 | EXPERIMENTAL SETUP

The experimental setup is illustrated in Figure 2, which consists of a sensing coil, a target, an X-Y-Z manual travel translation stage (10 μ m resolution, THORLABS Inc.), and an LCR-Meter (E4980A1-030, Keysight technologies). To verify that the method is valid for targets with complex and irregular shapes, a target mimicking the shape of a turbine blade was selected.

To validate that the algorithm and calibration method can be applied to sensing coils of different sizes, three planar coils with

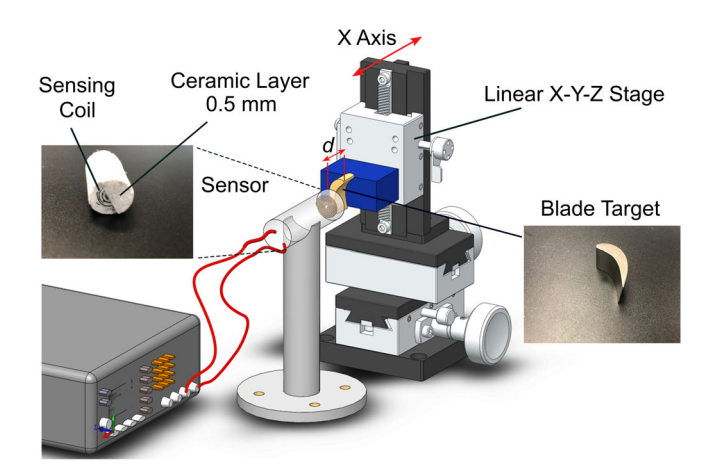


FIGURE 2 Experimental setup of the gap measurement for a narrow and irregular target

different geometries were fabricated using copper wires with insulated coating (18 Gauge, Solid Round Copper, Essex). The sizes of the coils are listed in Table 1. Each sensing coil was packaged with a ceramic protection layer (645-N, Ceramacast). The thickness of the ceramic layer is approximately 500 μ m, protecting the sensing coil. Four targets with the same geometry and different materials (titanium, zinc, aluminum, and copper), were tested to analyse the effect of the material/conductivity variations. The conductivities of these four materials vary from 0.75×10^6 to 59.95×10^6 S/m covering all the conductivities of the commonly-used metallic materials. The targets employed in the tests (Figure 3) mimic a gas turbine blade, whose geometry and dimensions are given in Figure 3(b) [30]. The targets were manufactured with a CNC machine (VF-1, Haas Automation Inc.). The thickness of the target is 13.03 mm, which is much larger than the maximum full penetration depth of the four materials (Cu, Al, Zn, and Ti) at 1 MHz [21].

The gap was adjusted by the X-Y-Z stage. The inductance of the sensing coil was measured using the LCR meter at various gaps.

Before the gap measurement tests, the phase angles of the three coils were measured under three different excitation frequencies (0.5, 1, and 2 MHz). Results showed that the phase angles of three coils were all larger than 85 degrees, implying that the coil inductance dominates the impedance of each coil. Thus, the serial R-L mathematical model can be applied within the working frequencies (0.5–2 MHz). Note that the excitation frequency in experience was chosen to be 1 MHz, the commonly working frequency of planar inductive sensors [31]. The base inductances, L_C , for the three sensing coils were measured with a 1 MHz excitation. The measured L_C were 1.601, 1.248, and 0.923 μ H.

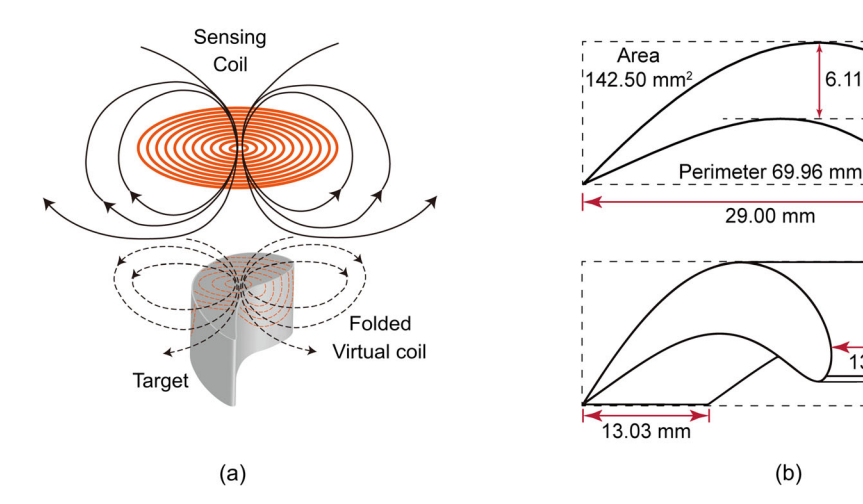
4 | RESULTS AND DISCUSSIONS

4.1 | Calibration

The equivalent inductance of each sensing coil was measured when the target was moved closer to or away from the

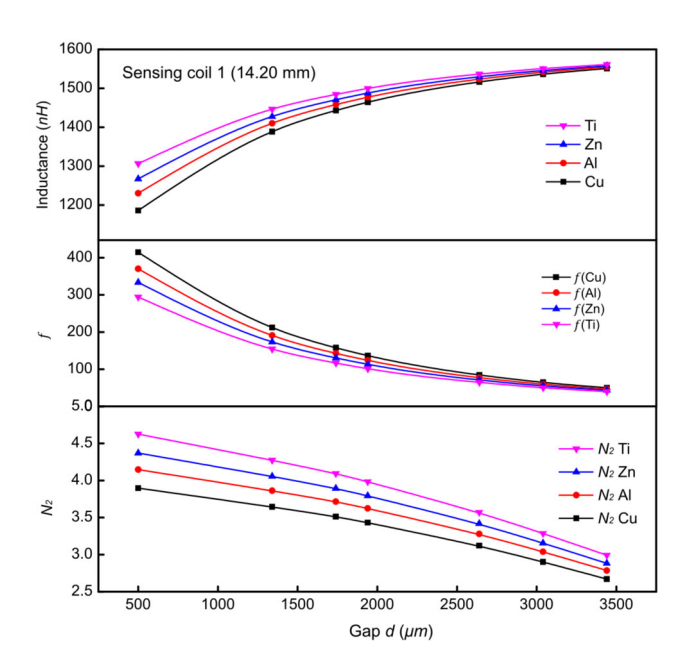
TABLE 1	The geometries and the excitation voltage/frequency of the three coils employed in experime	ents
IADLE	The geometries and the excitation voltage, frequency of the tiffee constitutioned in experime	CIILO

	Inner dia	Outer dia	# of turns	Excitation voltage/frequency	Base inductance
Coil 1	2.0 mm	14.20 mm	10	1 V / 1 MHz	1.601 μH
Coil 2	2.0 mm	12.92 mm	8	$1~\mathrm{V}$ / $1~\mathrm{MHz}$	$1.248\mu\mathrm{H}$
Coil 3	2.0 mm	9.02 mm	6	$1~\mathrm{V}$ / $1~\mathrm{MHz}$	$0.923\mu\mathrm{H}$



Working principle of blade target gap measurement and the design of blade-shaped target. (a) Schematic sketch of the gap measurement configuration between a sensing coil and a blade-shaped target. (b) Side view and isometric view of the blade target

sensing coil. Seven d values (Shown in Figure 4) ranging from 500 to 3600 μ m were used to establish the relation between the inductance change and d. All three coils were measured with four targets (with the same geometry) made of titanium, zinc, aluminum, and copper. Figure 4 (top) demonstrates the induc-



Measured inductance, calculated f function (in Equation (5)), and calculated N_2 of sensing coil 1 (14.20 mm) as a function of the gap d for four targets made of different materials (titanium, zinc, aluminum, and copper)

tance variations of sensing coil 1, suggesting that the inductance increases with an increase of gap due to the decrease of the mutual inductance between the sensor and the target. The inductance of the connection wire was minimized by reducing the wire length between the LCR and the sensing coil. Figure 4 (middle) shows the relation of f in Equation (5) as a function of gap d, where $f = L_C - L$. Then, all the known parameters d, r_1 , r_2 , N_1 , f, and L_C , were applied to Equation (5) to solve N_2 by the bi-section method, using the measured inductance L. A relation between N_2 and d of sensing coil 1 (14.20 mm in diameter) was established for the four targets, as shown in Figure 4 (bottom). Thus, with an increasing gap d, N_2 is decreased, reflecting the decrease in mutual inductance (or eddy current). In addition, the higher the conductivity of the material, the larger the value of N_2 since the eddy current increases with an increase of conductivity.

6.11 mm

13.03 mm

12.21 mm

Subsequently, we created a relation between the turn ratio (N_1/N_2) and the gap (d). N_2 versus d curves for sensing coil 2 and 3 were also obtained by repeating the same procedure, which can be converted to turn ratio to gap curves (N_1 values of sensing coil 2 and 3 are 6 and 8). The turn ratio (N_1/N_2) to gap (d) curves are defined as the calibration curves. Each sensing coil was tested with four targets made of different materials. Figure 5(a), 6(a), and 7(a) show the calibration curves of the three sensing coils of different sizes. For irregular and narrow targets, the calibration curves are parallel when changing materials. Thus, a base calibration curve can be established for a reference material, and the calibration curves for targets made of a different materials can be calculated by adding a constant C to

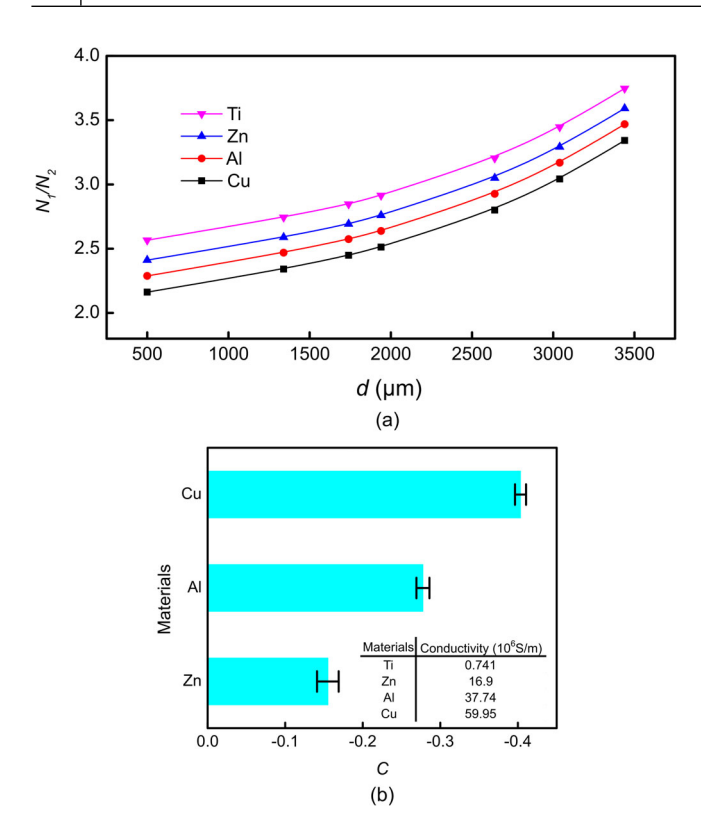


FIGURE 5 N_1/N_2 curves and constant C of four different target materials for coil 1. (a) N_1/N_2 curves obtained from sensing coil 1 for four different target materials. (b) Constant C for the four target materials with sensing coil 1

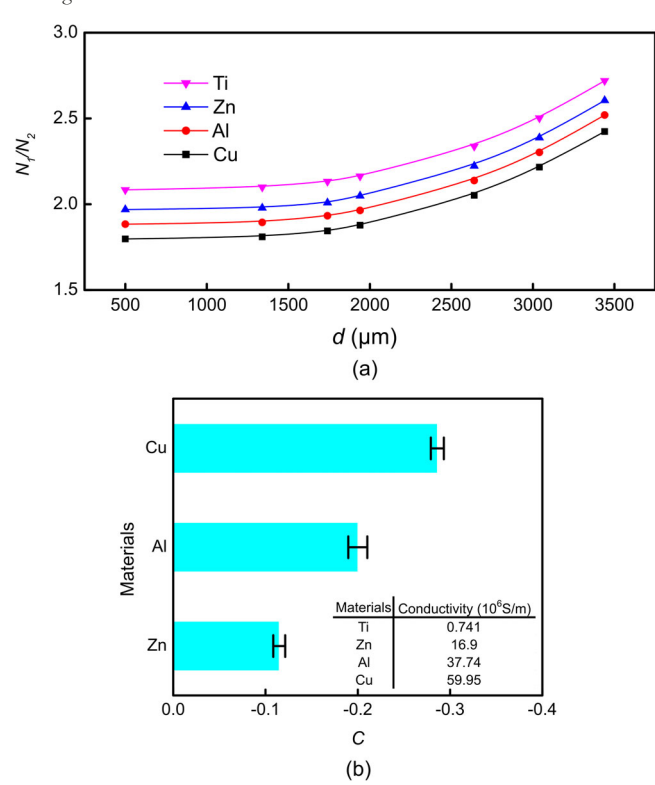


FIGURE 6 N_1/N_2 curves and constant C of four different target materials for coil 2. (a) N_1/N_2 curves obtained from sensing coil 2 for four different target materials. (b) Constant C for the four target materials with sensing coil 2

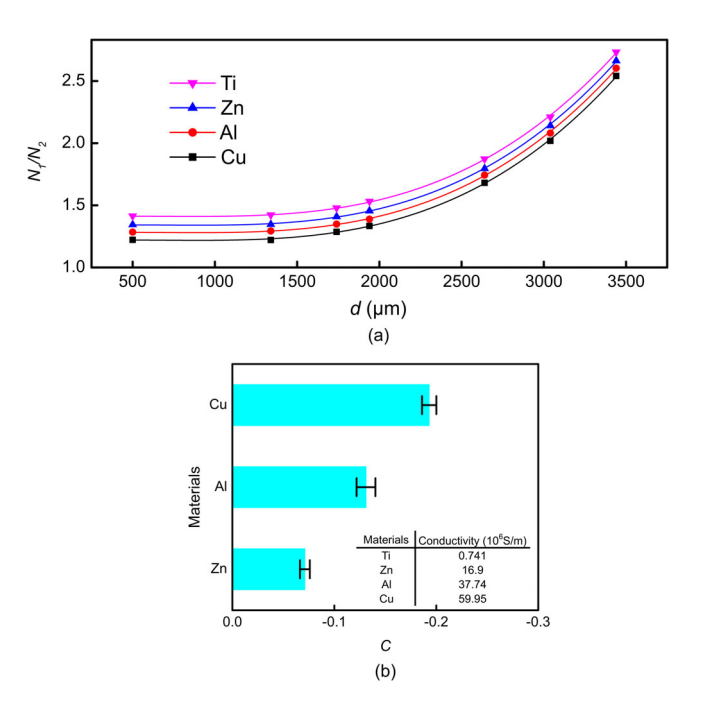


FIGURE 7 N_1/N_2 curves and constant C values of four different target materials for coil 3. (a) N_1/N_2 curves obtained from sensing coil 3 for four different target materials. (b) Constant C for the four target materials with sensing coil 3

the base curve. A similar phenomenon was found when using a planar coil to measure the gap from infinite plate targets made of different materials in our prior work [11]. Note that the titanium is used as the base material since it has to lowest N_1/N_2 value among the four materials. The constant C is the N_1/N_2 differences between the base material and another target material.

$$C = \left(\frac{N_1}{N_2}\right)_{Target} - \left(\frac{N_1}{N_2}\right)_{Base} \tag{6}$$

The C values and standard variations for the three coils are shown in Figure 5(b), 6(b), and 7(b), and are listed in Table 2. The variations in C are relatively small. The larger the sensing coil, the larger C is. A small sensing coil has a small value of C. The trend is in agreement with that for large plate targets.

Once the base calibration curve of a sensing coil for one material is obtained, the calibration curves for other materials can be obtained by adding a constant C to that base curve. The value of C for different materials and sensing coil combinations can be found in Table 2.

The process to establish a set of calibration curve for different materials is shown in Figure 8. To determine the constant C value, the following procedure is followed. First, the inductance of the sensing coil is measured at multiple known gaps (e.g. 7 gaps between 500 and 3600 μ m). The number of turns of the virtual coil can then be calculated with Equation (5). The base curve is then obtained through the relation between the turn ratio and the gap. To generate a calibration curve for another material, a target of that material only needs to be measured

TABLE 2 The value of C of three coils for the blade target

	Coil 1 (14.20 mm)	Coil 2 (12.92 mm)	Coil 3 (9.02 mm)
C (Zinc)	-0.1550 ± 0.0142	-0.1149 ± 0.0065	-0.0711 ± 0.0049
C (Aluminium)	-0.2776 ± 0.0084	-0.2001 ± 0.0103	-0.1310 ± 0.0093
C (Copper)	-0.4034 ± 0.0071	-0.2862 ± 0.0070	-0.1931 ± 0.0069

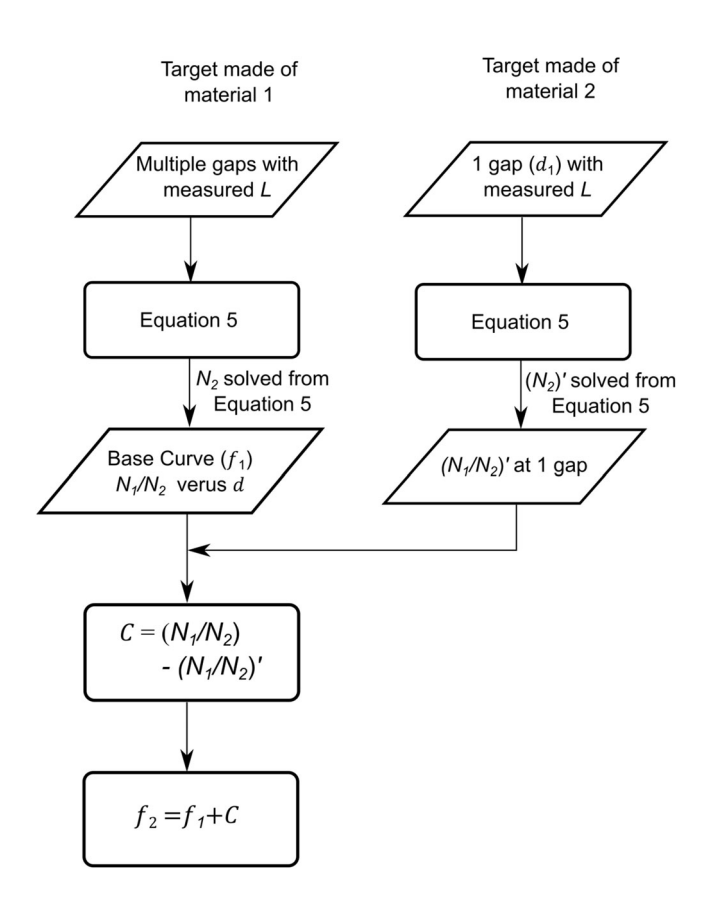


FIGURE 8 Flow chart of obtaining a set of calibration curves for targets made of different materials

at one gap. Again, the number of turns of the virtual coil can be determined for the new material with Equation (5). Finally, by calculating the difference between the turn ratios of the two materials at the measured gap, the constant C is acquired. By adding this constant C to the original base curve, the calibration curve for the new material is established.

Next, we evaluated the gap measurement accuracy using the calibration method. We selected the calibration curve for titanium as the base calibration curve, and obtained the calibration curve for the zinc, aluminum, and copper targets by adding the constant *C* values listed in Table 2.

4.2 | Error analysis

To estimate the accuracy of the calibration method, approximately 20 gap values ranging from 500 to 3600 μ m were tested for each blade target. From the calibration curves listed above,

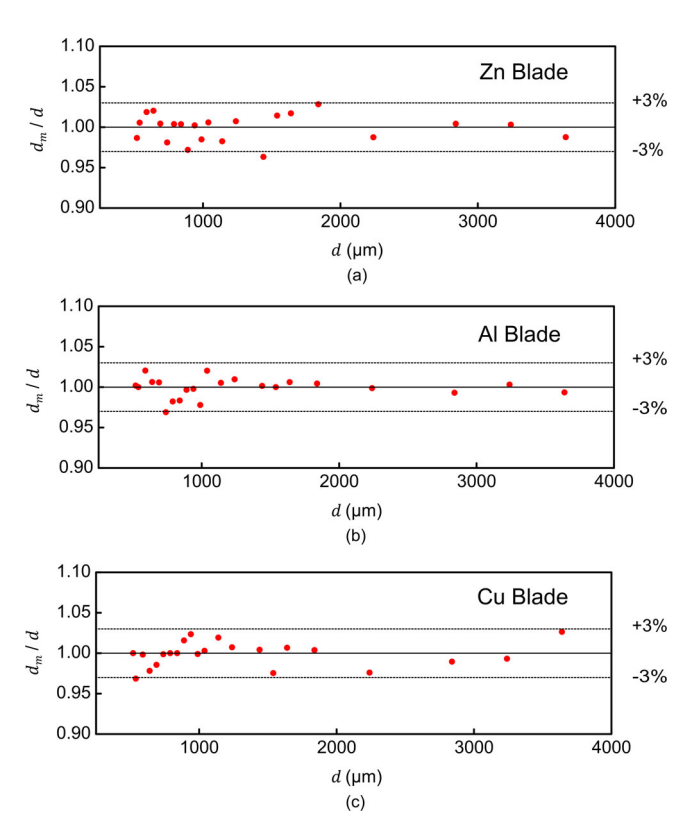


FIGURE 9 Ratios of the measured gap (d_m) over the real gap (d) between sensing coil 1 and the irregular blade targets made of (a) zinc, (b) aluminum, and (c) copper. The maximum errors for the zinc, aluminum, and copper targets were 3.681%, 3.108%. and 3.148%, respectively

the gap d can be determined from the measured inductance. The ratios between the measured gaps (d_m) and the real gaps (d) were also calculated, and are plotted in Figures 9, 10 and 11.

For sensing coil 1, the maximum error of the zinc blade was 3.681% when $d=1440~\mu m$ (Figure 9(a)). For the aluminum blade (Figure 9(b)), the maximum error was 3.108% at $d=740~\mu m$. When switching to a copper blade (Figure 9(c)), the maximum error was 3.148% when $d=540~\mu m$. Figure 10(a-c) shows the accuracy test results of sensing coil 2. The maximum error was 3.703% when $d=540~\mu m$ with an aluminum blade (Figure 10(b)). The accuracy test results for coil 3 are shown in Figure 11(a-c). The maximum error was 3.269% at $d=520~\mu m$ for an aluminum blade (Figure 11(b)). Three factors are responsible for the errors: the $10~\mu m$ resolution of the XYZ stage when setting the gap, the truncating error when calculating N_2 with the bisection method, and the limited amount of data points when establishing the calibration curves for base materials [32].

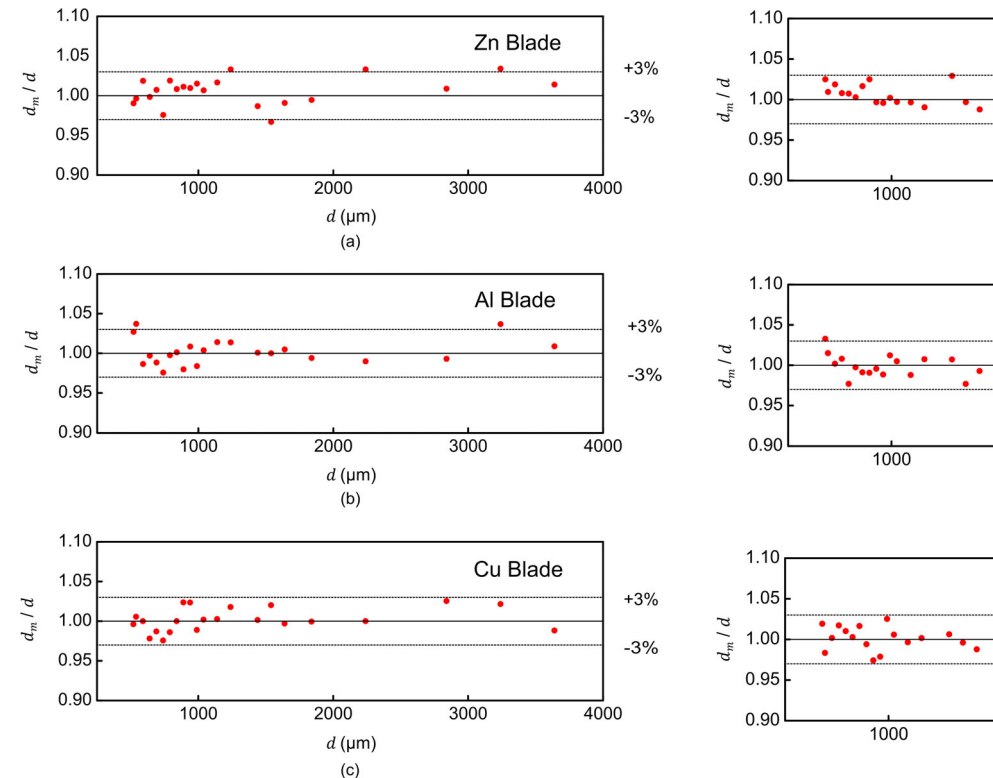


FIGURE 10 Ratios of the measured gap (d_m) over the real gap (d) between sensing coil 2 and the irregular blade targets made of (a) zinc, (b) aluminum, and (c) copper. The maximum errors for the zinc, aluminum, and copper targets were 3.395%, 3.703%, and 2.535%, respectively

For all measurements, the measured gap is in good agreement with the real gap, with relatively small measurement errors. The results indicate that there is no need to switch to a small sensing coil to measure the gaps from narrow or irregular targets. In the calibration process, only one base curve needs to be established for a given target; calibration curves for targets made by other materials can be obtained by adding constants to the base curve. The value of the constant C can be determined by measuring once at a known gap. This approach significantly simplifies the calibration when using planar inductive sensors to measure the gaps from a typical target when the target materials are changed.

4.3 | Discussions

For proximity sensors, the most commonly used calibration for industrial applications relies on the relation between the target distance and the sensor output (e.g. voltage or inductance) [33]. For example, when using a single-ended calibration method, when the target is moved from the closet position to the farthest position within the desired measurement range, the output voltage variations are recorded. In the calibration curve, the output voltage/inductance varies monotonically as the target distance changes [31]. However, the traditional calibration method is limited to a target whose shortest dimension (e.g. width) is at least twice (2.5–3 times as the general rule) the size of the outer diameter of the sensor. For measuring gaps from a smaller sized

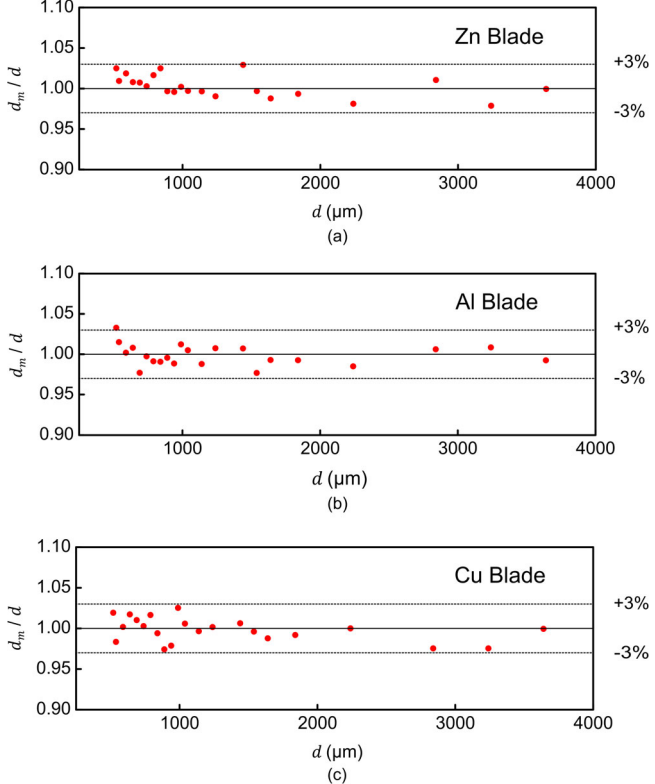


FIGURE 11 Ratios of the measured gap (d_m) over the real gap (d) between sensing coil 3 and the irregular blade targets made of (a) zinc, (b) aluminum, and (c) copper. The maximum errors for the zinc, aluminum, and copper targets were 2.916%, 3.269%, and 2.584%, respectively

target, a customized calibration has to be conducted [31]. Additionally, if the target material/conductivity is changed, recalibration is needed. Thus, when using a planar inductive sensor for gap measurements from narrow objects made of different materials, a set of customized calibrations has to be conducted, which are time consuming. The new method developed here can measure gaps from any irregular object made of various materials without tedious calibrations, but does not require for the planar coil sensor to be smaller than the objects. It provides great flexibilities in using planar inductive sensors of any size to measure the gaps of a larger variety of objects. Next we will discuss the utility of the method for a couple of critical applications.

As mentioned in introduction, there are challenges for applying planar inductive sensors in 3D printer build platform position monitoring, bandsaw blade deviation detection, and blade tip clearance monitoring. This method could play an indispensable role when using the same planar inductive sensors to measure the build platform positions, bad saw deviation, and the dynamic tip clearances of fan blades, made of different materials, with no need to recalibrate the sensor.

It is worth noting here that although there are several other non-contact measurement methods, including optical, capacitive, and ultrasonic, these methods have disadvantages for gap measurement, particularly from a typically shaped object. While optical sensors can measure gaps with high accuracy, it depends strongly upon the reflectivity (materials/colour) and

the orientation of the target [34]. A coarse or tilted surface is likely to cause measurement errors. In addition, optical sensors can be costly to install and are susceptible to external vibrations [35]. Capacitive sensors can also measure the gaps from narrow/irregular objects. However, the measurements are sensitive to environmental conditions such as the humidity, heat, and medium in the gap, which are often changing in applications such as 3-D printing tasks and fan blade tip clearance monitoring [36]. More importantly, capacitive sensors and particle concentrations will change frequently during printing tasks, making the capacitive sensor an inappropriate choice since it is sensitive to environmental changes. The accuracy is also affected by the parasitic capacitance problem [37], which varies when there is any change in environment or measurement setup. Ultrasonic proximity sensors also rely on the wave reflection from the target surface. The accuracy is affected by not only the surface properties of the reflective surface and environment conditions, but the diffraction at the edge of a narrow object [38]. In comparison, the planar inductive sensors are compact, easy to install, and less susceptible to environmental conditions [39]. Furthermore, when the target material is changed, using this new approach would avoid the need to recalibrate of the sensor. Therefore a planar inductive sensor would be suitable for the above applications.

In this article, we first established a new assumption that the magnetic flux is continuous at the boundary of the top and side surfaces, and can form a circle like shape when flipped from the side surface to the top surface. Thus, the sensor and target can be simplified to a coil-to-coil system. Second, we found that when using our approach, the calibrations for measuring gaps from narrow/irregular objects made of different materials are parallel, meaning that the calibration curve of a new material can be obtained just by adding a constant to a known curve. These findings greatly simplify the calibrations for many applications including, but not limited to, 3D printer build platform calibration, bandsaw blade deviation detection, and blade tip clearance monitoring. Finally, we expanded the measurement capability of planar inductive sensors, which can be used to measure gaps from narrow/irregular objects that are made of different materials with a simpler calibration process.

5 | CONCLUSION

In this study, we demonstrated the assumption that a planar inductive sensor measuring the gap from a narrow/irregular target can be modeled as a coil-to-coil system. Based on this assumption, we developed a new calibration method for planar inductive sensors. With this method, the gap from the object can be accurately measured without tedious calibration when the materials of the targets are changed. In our experiments, four blade-shaped targets made of four different materials, were used for demonstration. Three planar coils of different sizes were fabricated for testing. The inductance variation of each coil was measured for gaps ranging with four blade-like targets made of multiple materials. The established calibration curve for each coil shows that they are in parallel regardless of a typical

geometry. Hence, the calibration curves for a different material can be obtained by adding a constant C to the base curve. The accuracy tests show that the measurement error in the gap is within 3.703% with this new calibration methods. This method expands the gap or gap measurement capability for narrow or irregular targets without the need for complex calibrations. It is expected that this method can significantly reduce the calibration work to monitor the gap of targets in advanced industrial applications including 3D printer build platform calibration, bandsaw blade deviation detection, and blade tip clearance monitoring.

ACKNOWLEDGMENTS

This work was partially supported by NSF Awards #1940879 of USA.

REFERENCES

- Tumanski, S.: Induction coil sensors A review. Meas. Sci. Technol. 18, R31–R46 (2007)
- Yin, W., Peyton, A.J.: Thickness measurement of non-magnetic plates using multi-frequency eddy current sensors. NDT & E Int. 40, 43-48 (2007)
- Poliakine, J., Civet, Y., Perriard, Y.: Design and manufacturing of high inductance planar coils for small scale sensing applications. Proc. Eng. 168, 1127–1130 (2016)
- Hao, L., et al.: Inductive sensor based on nano-scale SQUIDs. IEEE Trans. Appl. Supercond. 15, 514–517 (2005)
- Guo, Y.X., et al.: Dimension-reduced analog-digital mixed measurement method of inductive proximity sensor. Sensors (Switzerland) 17(7), 1–24 (2017)
- Nabavi, M.R., Nihtianov, S.N.: Design strategies for eddy-current displacement sensor systems: Review and recommendations. IEEE Sens. J. 12, 3346–3355 (2012)
- Zuk, S., Pietrikova, A., Vehec, I.: Development of planar inductive sensor for proximity sensing based on LTCC. In: Proceedings of the International Spring Seminar on Electronics Technology. Pilsen, Czech Republic (2016)
- 8. Tian, G.Y., Zhao, Z.X., Baines, R.W.: The research of inhomogeneity in eddy current sensors. Sens. Actuators, A 69, 148–151 (1998)
- Yating, Y., Tuo, Y., Pingan, D.: A new eddy current displacement measuring instrument independent of sample electromagnetic properties. NDT & E Int. 48, 16–22 (2012)
- Wang, H., Li, W., Feng, Z.: Note: Eddy current displacement sensors independent of target conductivity. Rev. Sci. Instrum. (86(1), 1–4 2015)
- Jiao, D., et al. Measuring gaps using planar inductive sensors based on calculating mutual inductance. Sens. Actuators, A 295, 59–69 (2019)
- Ngo, T.D., et al.: Additive manufacturing (3D printing): A review of materials, methods, applications and challenges. Composites, Part B 143, 172–196 (2018)
- Bloome et al.: Controllable release build plate for 3d printer. US Patent 20170190120A1 (2016). https://patents.google.com/patent/ US20170190120?oq=patent:190120
- Evans, B.: Calibrating your printer. In: Practical 3D Printers. pp. 49– 74. Apress, New York (2012)
- Amza, C., Zapciu, A., Popescu, D.: Paste extruder—Hardware add-on for desktop 3D printers. Technologies 5(3), 50 (2017)
- Yang, X., Liu, C.R.: Machining titanium and its alloys. Mach. Sci. Technol. 3, 107–139 (1999)
- Gendraud, P., Roux, J.C., Bergheau, J.M.: Vibrations and stresses in band saws: A review of literature for application to the case of aluminiumcutting high-speed band saws. J. Mater. Process. Technol. 135, 109–116 (2003)
- Du, L., Zhu, X., Zhe, J.: A high sensitivity inductive sensor for blade tip clearance measurement. Smart Mater. Struct. 23(6), 065018 (2014)
- VanderKlok, A., Stamm, A., Xiao, X.: Fan-blade-out experiment at small scale. Exp. Technol. 40(6), 1479–1484 (2016)

- Rust, T.M., Steltz, W.G.: Titanium for steam turbine blades. JOM J. Miner. Metall. Mater. Soc. 34(9), 42–47 (1982)
- 21. Wang, H., Li, W., Feng, Z.: Noncontact thickness measurement of metal films using eddy-current sensors immune to distance variation. IEEE Trans. Instrum. Meas. (64(9), 2557–2564 2015)
- 22. Vyroubal, D.: Impedance of the eddy-current displacement probe: The transformer model. IEEE Trans. Instrum. Meas. 53, 384–391 (2004)
- Paese, E., et al.: Simplified mathematical modeling for an electromagnetic forming system with flat spiral coil as actuator. J. Braz. Soc. Mech. Sci. Eng. 33, 324–331 (2011)
- Wang, H., et al.: Ultrastable eddy current displacement sensor working in harsh temperature environments with comprehensive self-temperature compensation. Sens. Actuators, A (211, 98–104 2014)
- Babic, S., Akyel, C.: Improvement in calculation of the self- and mutual inductance of thin-wall solenoids and disk coils. IEEE Trans. Magn. 36, 1970–1975 (2000)
- Akyel, C., Babic, S.: Mutual inductance between coaxial circular coils of rectangular cross section and thin coaxial circular coils with constant current density in air (filament method). In: Proceedings of 6th WSEAS International Conference on Applications of Electrical Engineering. Istanbul, Turkey (2007)
- Conway, J.T.: Inductance calculations for noncoaxial coils using bessel functions. IEEE Trans. Magn. 43, 1023–1034 (2007)
- 28. Babic, S., Salon, S., Akyel, C.: The mutual inductance of two thin coaxial disk coils in air. IEEE Trans. Magn. 40, 822–825 (2004)
- Su, Y.P., Liu, X., Hui, S.Y.R.: Mutual inductance calculation of movable planar coils on parallel surfaces. IEEE Trans. Power Electron. 24, 1115– 1123 (2009)
- Dhivya, S., Karthikeyan, A.: Design and analysis of gas turbine blade with cooling. EAI Endorsed Transactions on Energy Web and Information Technologies 18(20), 1097–104 (2018)
- Products, P.: Inductive Technology Handbook. Kaman Precision Products /Measuring, Colorado Springs, CO (2012)
- Meeter, D.: Introduction to numerical analysis. Technometrics 8, 719, (1966)

- 33. Functionality and technology of inductive sensors. https://laumanstechniek.nl/nl/Inductive-sensors-functionality. Accessed September 10th, 2020.
- Regtien, P.P.L.: Accurate optical proximity detector. In: 7th IEEE Conference on Instrumentation and Measurement Technology. San Jose, CA, pp. 141–143 (1990)
- 35. Fu, Z., Lu, Y.-.C., Lai, J.J.: Recent advances in biosensors for nucleic acid and exosome detection. Chonnam Med. J. 55, 86, (2019)
- Oertel, B., Hübert, T., Heinze, D., Banach, U.: Capacitive sensor system for measurement of temperature and humidity. Fresenius J. Anal. Chem. 349, 391–393 (1994)
- Kung, J.T., Lee, H.S., Howe, R.T.: A digital readout technique for capacitive sensor applications. IEEE J. Solid-State Circuits 23, 972–977 (1988)
- Vladišauskas, A., Jakevičius, L.: Absorption of ultrasonic waves in air. Ultragarsas. 50(1), 46–49 (2004)
- Poliakine, J., Civet, Y., Perriard, Y.: Design and manufacturing of high inductance planar coils for small scale sensing applications. Proc. Eng. 168, 1127–1130 (2016)

SUPPORTING INFORMATION

Additional supporting information may be found online in the Supporting Information section at the end of the article.

How to cite this article: Jiao, D., et al.: A non-contact gap measurement method for narrow and irregular targets using inductive planar sensors with simple calibration. IET Sci. Meas. Technol.15, 710–718 (2021). https://doi.org/10.1049/smt2.12071